

Determining the Syringyl/Guaiacyl Lignin Ratio in the Vessel and Fiber Cell Walls of Transgenic *Populus* Plants

Allison K. Tolbert,[†] Tao Ma,[†] Udaya C. Kalluri,[†] and Arthur J. Ragauskas^{*,†,‡,§}

School of Chemistry and Biochemistry and Renewable Bioproducts Institute, Georgia Institute of Technology, Atlanta, Georgia 30332, United States

Supporting Information

ABSTRACT: Observation of the spatial lignin distribution throughout the plant cell wall provides insight into the physicochemical characteristics of lignocellulosic biomass. The distribution of syringyl (S) and guaiacyl (G) lignin in cell walls of a genetically modified *Populus deltoides* and its corresponding empty vector control were analyzed with time-of-flight secondary ion mass spectrometry (ToF-SIMS) and then mapped to determine the S/G lignin ratio of the sample surface and specific regions of interest (ROIs). The surface characterizations of transgenic cross-sections within 1 cm vertical distance of each other on the stem possess similar S/G lignin ratios. The analysis of the ROIs determined that there was a 50% decrease in the S/G lignin ratio of the transgenic xylem fiber cell walls.

1. INTRODUCTION

A better understanding of lignocellulosic biomass at the molecular level is necessary as the interest in the utilization of this resource increases.¹ The cell wall structure of lignocellulosic biomass is mainly composed of several biopolymers: cellulose, hemicellulose, and lignin. In particular, the structure of lignin varies depending upon the species of biomass, age, and its environment. Lignin is mainly composed of one to three monolignols, including coniferyl, sinapyl, and *p*-coumaryl alcohol; these alcohols yield lignin structural units of guaiacyl (G), syringyl (S), and *p*-hydroxyphenyl (H) connected through various ether and/or carbon–carbon linkages.² Lignin assists in binding adjacent cell walls together, helps to strengthen the structure of the plant cell wall, and facilitates in water transportation through its hydrophobic properties; it also happens to be one of the most recalcitrant chemical components within the plant cell wall, meaning that it is naturally resistant to chemical and biological degradation.³ The inherent recalcitrance presents an impediment to biological or chemical conversion of cellulose to biofuels and chemicals.

Scientists have made significant strides in overcoming the natural recalcitrance of biomass through genetic modification.⁴ They have routinely manipulated the biosynthetic pathways involved in forming the primary and secondary plant cell walls.^{4–6} The changes in biomass properties can be measured in morpho-chemico-anatomic characteristics, such as growth, cell structure, and amounts of cellulose, hemicellulose, and lignin.

Typically, biomass chemistry is characterized by bulk analysis, which can include cellulose crystallinity, cellulose and lignin molecular weight, degree of polymerization of cellulose, percentage of carbohydrates and Klason lignin, and syringyl/guaiacyl (S/G) lignin ratio. All of these techniques provide insight into the biomass and the impact that any chemical, physical, and/or biological treatments have on the biomass structures. Also, nuclear magnetic resonance (NMR) spectroscopy and mass spectrometry (MS) techniques have

advanced significantly in characterizing the structure of lignin.^{7–9}

The aforementioned bulk analyses, however, have a limited resolution at the cellular level. For example, distinguishing between the primary and secondary cell walls and the middle lamella, especially in intact *in situ* tissue samples, is challenging. Some surface characterization analyses can allow spatial distribution of cellulose and lignin in the plant cell walls to be observed with minimal damage to the biomass. Various methods have been used to determine the cell-specific distribution of lignin in biomass samples, including ultraviolet (UV) microscopy, Raman spectroscopy, and light microscopy.^{10–13} Time-of-flight secondary ion mass spectrometry (ToF-SIMS) is another analytical instrument that allows for the direct chemical mapping or chemical imaging of a sample at high spatial resolutions with minimal to no degradation. Not only does ToF-SIMS analysis provide two-dimensional mapping of the distribution of chemical fragmentations across the surface of biomass, but it also is capable of semi-quantitative measurement of cellulose and lignin.^{14–16} Recently, the distribution of S and G lignin on cross-sections of maple and poplar wood using ToF-SIMS was reported.^{17,18} These studies indicated that S lignin is predominately found within the fiber cell walls, while G lignin majorly contributes to the vessel walls, especially in early wood; this confirms the results using other instrumentation in previous studies and shows the accuracy of the ToF-SIMS analysis.^{17,18} The focus on distinguishing the S and G lignin in the biomass is important because of a correlation between sugar release and S/G ratios.¹⁹

Modification of the cellulose biosynthesis pathway can result in alterations to the lignocellulosic chemical composition in the plant cell walls. Detailed characterization of such genetically modified biomass samples can provide a greater understanding

Received: March 8, 2016

Revised: May 16, 2016



of the mechanisms of recalcitrance and help design strategies to improve accessibility of cellulose substrate for biofuel production. The changes to the chemical composition as a result of downregulation of the *PdKOR2* gene was studied in *Populus deltoides*.²⁰ The *PdKOR2* gene is a close sequence homologue of the *Arabidopsis* KORRIGAN (KOR) gene, an endo-1,4- β -glucanase, shown to be part of the cellulose biosynthesizing cellulose synthase complex.²¹ Bulk chemical analysis of transgenic *PdKOR2* RNAi plants showed that the suppression of the gene resulted in small but significant reduction in the ratio of S and G lignin units (S/G ratio).²⁰ The observation of stunted growth and significantly impacted secondary metabolism²⁰ led to an investigation of the effect of *PdKOR2* modification on cell-wall-specific properties. Using the surface characterization analysis, it is possible to determine if there are additional, currently undetected changes occurring in the plant cell walls, especially with regard to the S/G lignin ratio of particular cell wall types. Here, we applied the ToF-SIMS technique to detect S/G lignin ratio changes in xylem vessel and fiber cell walls between control and transgenic *P. deltoides* stem samples.

2. EXPERIMENTAL SECTION

2.1. Materials. The cellulose biosynthesis pathway of *P. deltoides* was altered by RNAi mediated downregulation of *PdKOR2* gene, resulting in the transgenic sample.²⁰ Transgenic *P. deltoides* and an empty vector control plant, referred to as control or control sample, were then grown in Oak Ridge National Laboratory (ORNL) greenhouses at 25 °C with 16 h daylight for approximately 180 days;²² additional details regarding the genetic modification and plant growth are described in the study by Kalluri et al.²⁰

2.2. Chemical Bulk Analysis. The steps used to analyze the bulk chemistry of the control and transgenic samples are described in detail in the study by Kalluri et al.²⁰ Briefly, the National Renewable Energy Laboratory, Golden, CO, analyzed the lignin and S/G ratio of a 4 mg stem sample (control and transgenic) by pyrolysis molecular beam mass spectrometry (MBMS).²⁰ Extractive-free control and transgenic samples (5 mg) were treated with sulfuric acid, diluted with deionized (DI) water, and autoclaved to solubilize the biomass carbohydrates. The glucose and xylose percentages were quantified using sugar standards run by high-performance liquid chromatography.

2.3. Cryotome Section of Poplar Stem. The juvenile poplar stem (approximately 2 cm in diameter) was cross-sectioned to 80 μ m thick slices using a LEICA SM 3050S cryostat instrument with embedding material (OCT compound, Tissue-TEK) and a disposable steel blade. The disposable steel blade was wiped with methylene chloride, hexane, acetone, and alcohol to remove any lubricants on its surface prior to installation into the instrument. The poplar stem was attached to a metal plate using a small amount of embedding material on the base and sides (no more than 5 mm). The chamber temperature for the instrument was from approximately -5 to -8 °C, and the cutting speed was controlled manually.¹⁶

2.4. Extractive-Free Poplar. Extractive-free poplar samples were prepared by Soxhlet extraction. The cross-sections were refluxed for 4 h in a Foss Soxtec 2050 (FOSS Analytical, Höganäs, Sweden) with dichloromethane (\sim 250 mL).

2.5. ToF-SIMS Analysis. An ION-TOF TOF-SIMS V (ION-TOF, Münster, Germany) instrument (lateral resolution, \sim 300 nm; vertical resolution, \sim 2 nm) was used to analyze the poplar cross-section using a Bi⁺ primary ion gun in positive-ion mode at 25 kV. The samples were rastered over a 100 or 200 μ m² area (256 \times 256 pixels) for 600 scans to form the total ion images. Further analysis of the images allowed for S lignin (m/z 167 and 181), G lignin (m/z 137 and 151), and cellulose (m/z 127 and 145) fragmentation ions to be selected from the mass spectra, assigned a specific color, and overlaid on another image. In this case, cellulose and lignin images (green) were overlaid on the total ion image (red), while G lignin (green) was overlaid on the S lignin

image (red). The regions of interests (ROIs) were selected manually on the total ion images, which allowed for the regeneration of the ToF-SIMS spectra and normalized ion intensities for each ROI; refer to Figure S1 of the Supporting Information for a representative image spectrum of the control sample and a brief description of the ROI analysis. All S/G lignin ratios were computationally analyzed on the basis of the normalized ion intensities for the fragmentation ion. All analyses of the ToF-SIMS data were conducted using the ION-TOF measurement program.

3. RESULTS AND DISCUSSION

Kalluri et al. recently studied the effects of downregulating the *PdKOR2* gene on cell wall, growth, and physiological properties in *P. deltoides*.²⁰ They reported a slight but important reduction in cellulose (1.4–1.8%) and lignin (0.9–1.9%) contents and S/G lignin ratios (9.8–16.0%) in *PdKOR2* transgenic lines relative to control plants (Table 1). A previous study using

Table 1. Major Chemical Components for Control and KOR2 Transgenic Lines²⁰

line	glucose (%)	xylose (%)	lignin (%)	S/G ratio ^a
control	34.7 \pm 0.4	15.0 \pm 0.2	25.8 \pm 0.2	1.2
KOR2-1	33.3 \pm 0.3	15.6 \pm 0.4	23.9 \pm 0.6	1.0
KOR2-2	32.9 \pm 0.5	14.9 \pm 0.1	24.9 \pm 0.4	1.1

^aStandard deviation < 0.01.

Populus trichocarpa showed that, for S/G ratios less than 2.0, there are negative correlations between sugar release, specifically glucose release, and the lignin content.¹⁹ It was determined that sugar release is dependent upon the S/G lignin ratio or the lignin composition.¹⁹

In this study, the surface of a similar *PdKOR2* line and control stem cross-sections were characterized using the spatial mapping capabilities of ToF-SIMS to obtain a better understanding of the effects of the genetic modification on biomass properties. The total ion image for the control and transgenic samples can be seen in panels a and b of Figure 1 along with their corresponding cellulose (panels c and d of Figure 1) and lignin (panels e and f of Figure 1) mapping. To highlight the locations on the cell walls where cellulose and lignin fragmentation ions were detected, the ions for those chemical components were assigned a specific color, in this case green. Separately, the green cellulose ion image and the green lignin ion image were overlaid on the total ion image (red). The benefit of this type of mapping is to determine the locations for high intensities of cellulose and lignin. Consider the transgenic lignin image (Figure 1f) and observe the high intensities of lignin in the middle lamella and cell corners, which are typical locations for significant concentrations of lignin. This indicates that, while the overall lignin percentage does decrease slightly for the transgenic (Table 1), the genetic modifications do not cause lignin to form in atypical areas or cause ectopic deposition of lignin.

The next step in the analysis was to determine if the S/G ratios on the surface decrease for the transgenic compared to the control and if it matches the trend seen in the bulk analysis (Table 1). The ToF-SIMS S/G lignin ratio for the control was determined to be 1.1, which was close to that corresponding to the value in the bulk chemistry analysis (1.2); the ToF-SIMS S/G ratio for transgenic was determined to be 0.8, which is lower than the bulk value (1.0–1.1). This 20–27% difference in S/G ratios for the transgenic can be attributed to ToF-SIMS detecting only the chemical components on the surface of the

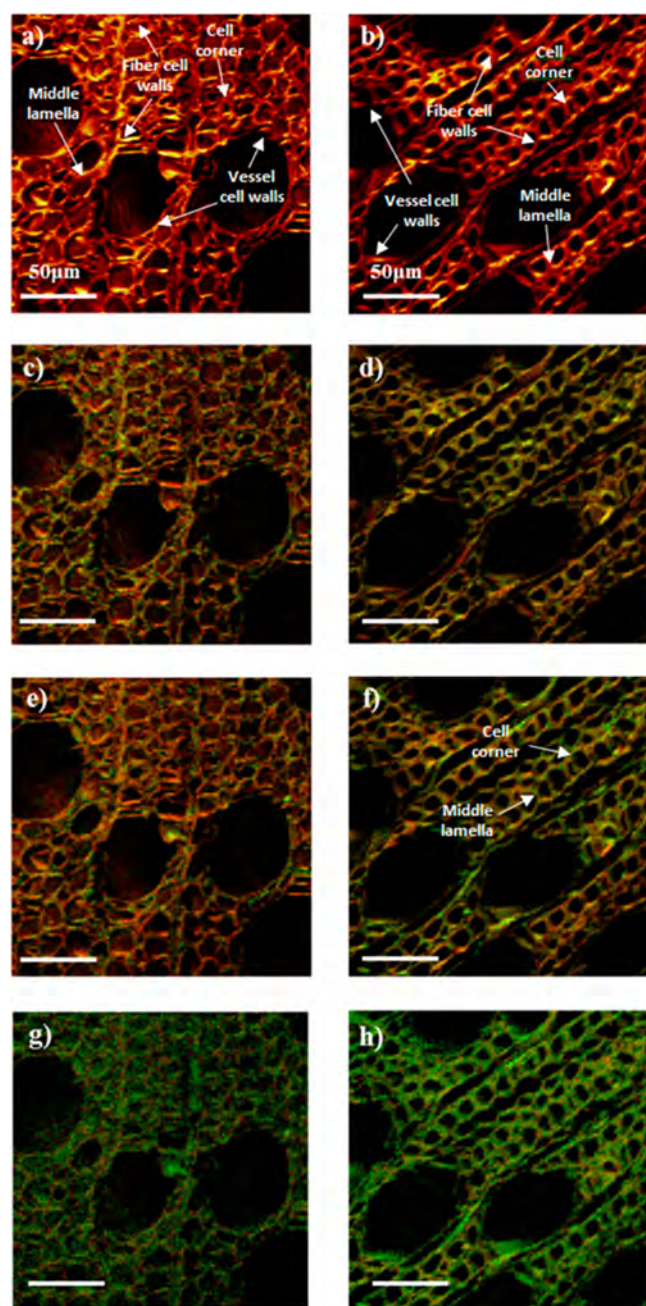


Figure 1. ToF-SIMS images of (a and b) total ion, (c and d) cellulose, (e and f) lignin, and (g and h) G lignin overlaid on S lignin for the control (a, c, e, and g) and transgenic (b, d, f, and h) cross-sections, 80 μm thick. Green cellulose and lignin ion images were overlaid on the total ion image (red) (c–f). The G lignin (green) was overlaid on the S lignin (red) (g and h). Scale bar = 50 μm .

sample and the natural heterogeneity of the biomass. The lower overall S/G ratio of the transgenic (Figure 1b) compared to the control (Figure 1a) may also be impacted by a change in amounts of G and S lignin in the samples, for example, an increase in G lignin, a decrease in S lignin, or a combination of the two. The G lignin images for the control and the transgenic cross-sections both show high amounts of G lignin (panels g and h of Figure 1). The transgenic G lignin (Figure 1h) appears to be denser in area coverage than the control (Figure 1g), meaning that there are fewer red pixels representing S lignin. This indicates that both an increase in G lignin and a decrease

in S lignin occurred on the surface of the transgenic *Populus* samples.

Finally, it is important to look closer at the cell walls to determine if the change in lignin composition is concentrated in the vessel cells, fiber cells, or both. This was accomplished by selecting specific ROIs on the ToF-SIMS images and determining the corresponding S/G ratios for each location. The ROIs in Figure 2 are represented by white squares with an

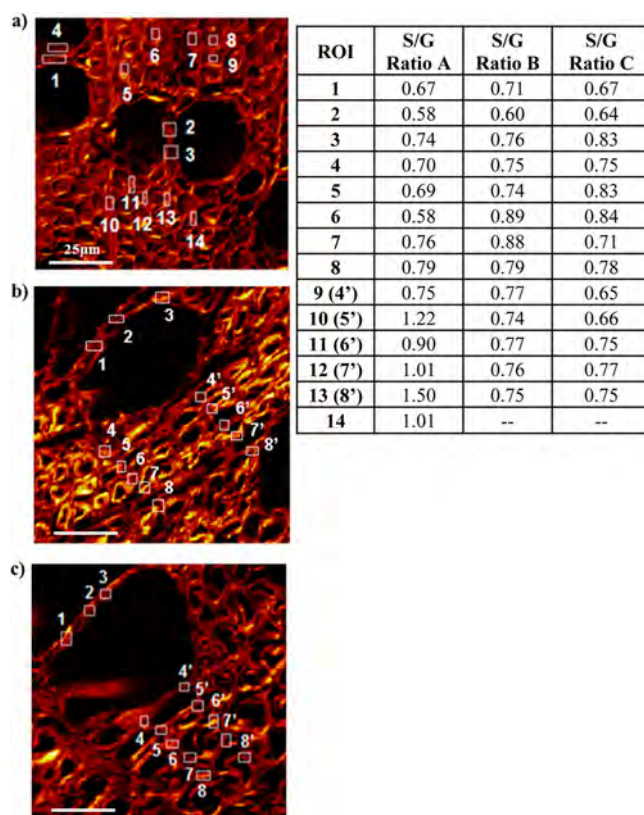


Figure 2. ToF-SIMS images for (a) control, (b) transgenic sample 1, and (c) transgenic sample 2 with ROIs (white boxes). Transgenic samples 1 and 2 were harvested within 1 cm of each other. Scale bar = 25 μm . The table reports S/G ratios for (a) control, (b) transgenic sample 1, and (c) transgenic sample 2 for the ROIs numbered in the corresponding images.

identifying number that corresponds to the S/G ratios in the table to the right of the images. The control sample (Figure 2a) has average S/G ratios of 0.66 and 1.13 for its vessel (ROI 1–3) and fiber (ROI 10–14) cells, respectively. The next two samples (panels b and c of Figure 2) are transgenic cross-sections cut within 1 cm of each other. Both samples have vessel ROI (1–3) and fiber ROIs (4–8 and 4'–8') with S/G lignin ratio values listed in the table (Figure 2). The average S/G vessel ratios for transgenic samples 1 and 2 are 0.69 and 0.71, respectively. Likewise, the average fiber S/G ratio value is 0.78 for transgenic sample 1 and 0.75 for transgenic sample 2. The purpose of analyzing two transgenic cross-sections was to prove that the S/G lignin ratios for vessel and fiber cells do not vary significantly within a small vertical distance from each other.

When the transgenic ToF-SIMS average S/G ratio values are compared to that of the control, the vessel cell walls only indicate a 5–7% value difference (Table 2). The change in the fiber cell average S/G ratio is, however, more pronounced, with the control fiber cells having between 45 and 51% average

Table 2. ToF-SIMS Vessel and Fiber S/G Ratios for the Three *P. deltooides* Plant Genotypes and Wild-Type *P. trichocarpa*

	vessel S/G ratio	fiber S/G ratio
control	0.66	1.13
transgenic sample 1	0.69	0.78
transgenic sample 2	0.71	0.75
<i>P. trichocarpa</i> ¹⁷	0.70	1.10

higher S/G lignin compared to the transgenic. The overall lower S/G ratio in the vessel cell walls versus the fiber cell walls agrees with the findings by Saito et al.; they determined that the G lignin is integrated in the cell walls during the “early to late stages of xylem differentiation”, explaining why more G lignin can be found in the early-forming vessel cell walls.¹⁸ Zhou et al. showed that *P. trichocarpa* cross-stems had higher S/G ratios for fiber cell walls (1.1) than vessel cell walls (0.7).¹⁷ These data correlate well with the control sample average S/G ratio for the vessel and fiber cell walls and the average vessel cell wall S/G ratio for the transgenic (Table 2). The lower fiber cell wall S/G ratio in the transgenic samples indicates that this is where the change in the overall S/G ratio value is occurring.

4. CONCLUSION

ToF-SIMS is a useful tool for mapping out the chemical changes within the plant cell wall, specifically with regard to the S/G lignin ratio for vessel and fiber cell walls. The impact in downregulating the *PdKOR2* gene in the transgenic plant was in almost a 50% decrease in the S/G lignin ratio on the fiber cell walls, while the vessel cell walls reported an increase in the S/G lignin ratio to be less than 10%. This resulted in the transgenic overall S/G lignin ratio to be less than the control, which is in agreement with the bulk S/G lignin ratio. This significant change in the S/G lignin ratio in the transgenic *PdKOR2* RNAi fiber cell walls, which was not detected by bulk analysis, could be a contributor to the stunted plant growth properties.²⁰

■ ASSOCIATED CONTENT

Supporting Information

The Supporting Information is available free of charge on the ACS Publications website at DOI: [10.1021/acs.energyfuels.6b00560](https://doi.org/10.1021/acs.energyfuels.6b00560).

ToF-SIMS images spectra for (a) G lignin and (b) S lignin for the control sample (Figure S1) (PDF)

■ AUTHOR INFORMATION

Corresponding Author

*Address: Oak Ridge National Laboratory, Post Office Box 2008 MS6341, Oak Ridge, Tennessee 37831-6341, United States. Telephone: 1-865-576-0635. E-mail: aragausk@utk.edu.

Present Addresses

†Allison K. Tolbert, Tao Ma, Udaya C. Kalluri, and Arthur J. Ragauskas: BioEnergy Science Center (BESC), Biosciences Division, Oak Ridge National Laboratory, Oak Ridge, Tennessee 37830, United States.

‡Arthur J. Ragauskas: University of Tennessee (UT)–Oak Ridge National Laboratory (ORNL) Joint Institute of Biological Science, Biosciences Division, Oak Ridge National Laboratory, Oak Ridge, Tennessee 37831, United States.

§Arthur J. Ragauskas: Department of Chemical and Biomolecular Engineering and Department of Forestry, Wildlife, and Fisheries, University of Tennessee, Knoxville, Tennessee 37996, United States.

Notes

The authors declare no competing financial interest.

■ ACKNOWLEDGMENTS

This manuscript has been authored by University of Tennessee (UT)–Battelle, LLC under Contract DE-AC05-00OR22725 with the U.S. Department of Energy. The BioEnergy Science Center is supported by the Office of Biological and Environmental Research in the U.S. Department of Energy. Mass spectrometry analysis was carried out by the U.S. Department of Energy Office of Biological and Environmental Research supported by the BioEnergy Research Center proteomics pipeline. The publisher, by accepting the article for publication, acknowledges that the United States Government retains a non-exclusive, paid-up, irrevocable, worldwide license to publish or reproduce the published form of this manuscript or allow others to do so for United States Government purposes. The U.S. Department of Energy will provide public access to these results of federally sponsored research in accordance with the DOE Public Access Plan (<http://energy.gov/downloads/doe-public-access-plan>). Allison K. Tolbert is grateful for the financial support from the Paper Science and Engineering (PSE) fellowship program at the Renewable Bioproducts Institute at Georgia Institute of Technology.

■ NOMENCLATURE

S lignin = syringyl lignin
G lignin = guaiacyl lignin
S/G ratio = syringyl/guaiacyl ratio

■ REFERENCES

- Ragauskas, A. J.; Williams, C. K.; Davison, B. H.; Britovsek, G.; Cairney, J.; Eckert, C. A.; Frederick, W. J.; Hallett, J. P.; Leak, D. J.; Liotta, C. L. *Science* **2006**, *311* (5760), 484–489.
- Weng, J. K.; Chapple, C. *New Phytol.* **2010**, *187* (2), 273–285.
- Tolbert, A.; Akinoshio, H.; Khunsupat, R.; Naskar, A. K.; Ragauskas, A. J. *Biofuels, Bioprod. Biorefin.* **2014**, *8* (6), 836–856.
- Kalluri, U. C.; Yin, H.; Yang, X.; Davison, B. H. *Plant Biotechnol. J.* **2014**, *12* (9), 1207–1216.
- Yang, F.; Mitra, P.; Zhang, L.; Prak, L.; Verherbruggen, Y.; Kim, J. S.; Sun, L.; Zheng, K.; Tang, K.; Auer, M.; Scheller, H. V.; Loqué, D. *Plant Biotechnol. J.* **2013**, *11* (3), 325–335.
- McCann, M. C.; Carpita, N. C. *Curr. Opin. Plant Biol.* **2008**, *11* (3), 314–320.
- Capanema, E. A.; Balakshin, M. Y.; Kadla, J. F. *J. Agric. Food Chem.* **2004**, *52* (7), 1850–1860.
- Ralph, J.; Lapierre, C.; Marita, J. M.; Kim, H.; Lu, F.; Hatfield, R. D.; Ralph, S.; Chapple, C.; Franke, R.; Hemm, M. R.; Van Doorselaere, J.; Sederoff, R. R.; O'Malley, D. M.; Scott, J. T.; MacKay, J. J.; Yahiaoui, N.; Boudet, A.-M.; Pean, M.; Pilate, G.; Jouanin, L.; Boerjan, W. *Phytochemistry* **2001**, *57* (6), 993–1003.
- Reale, S.; Di Tullio, A.; Spredi, N.; De Angelis, F. *Mass Spectrom. Rev.* **2004**, *23* (2), 87–126.
- Fergus, B.; Goring, D. *Holzforchung* **1970**, *24* (4), 118–124.
- Musha, Y.; Goring, D. *Wood Sci. Technol.* **1975**, *9* (1), 45–58.
- Schmidt, M.; Schwartzberg, A.; Perera, P.; Weber-Bargioni, A.; Carroll, A.; Sarkar, P.; Bosneaga, E.; Urban, J.; Song, J.; Balakshin, M.; Capanema, E. A.; Auer, M.; Adams, P. D.; Chiang, V. L.; Schuck, P. *J. Planta* **2009**, *230* (3), 589–597.
- Watanabe, Y.; Kojima, Y.; Ona, T.; Asada, T.; Sano, Y.; Fukazawa, K.; Funada, R. *IAWA Journal* **2004**, *25* (3), 283–295.

- (14) Saito, K.; Kato, T.; Tsuji, Y.; Fukushima, K. *Biomacromolecules* **2005**, *6* (2), 678–683.
- (15) Goacher, R. E.; Jeremic, D.; Master, E. R. *Anal. Chem.* **2011**, *83* (3), 804–812.
- (16) Jung, S.; Foston, M.; Sullards, M. C.; Ragauskas, A. J. *Energy Fuels* **2010**, *24* (2), 1347–1357.
- (17) Zhou, C.; Li, Q.; Chiang, V. L.; Lucia, L. A.; Griffis, D. P. *Anal. Chem.* **2011**, *83* (18), 7020–7026.
- (18) Saito, K.; Watanabe, Y.; Shirakawa, M.; Matsushita, Y.; Imai, T.; Koike, T.; Sano, Y.; Funada, R.; Fukazawa, K.; Fukushima, K. *Plant J.* **2012**, *69* (3), 542–552.
- (19) Studer, M. H.; DeMartini, J. D.; Davis, M. F.; Sykes, R. W.; Davison, B.; Keller, M.; Tuskan, G. A.; Wyman, C. E. *Proc. Natl. Acad. Sci. U. S. A.* **2011**, *108* (15), 6300–6305.
- (20) Kalluri, U. C.; Payyavula, R.; Labbé, J.; Engle, N.; Bali, G.; Jawdy, S.; Sykes, R.; Ragauskas, A.; Tuskan, G.; Tschaplinski, T. Down-regulation of an endo- β -1,4-glucanase gene impacts carbon partitioning, mycorrhizal colonization and biomass production. *Frontiers in Plant Science* **2016**, In review.
- (21) Vain, T.; Crowell, E. F.; Timpano, H.; Biot, E.; Desprez, T.; Mansoori, N.; Trindade, L. M.; Pagant, S.; Robert, S.; Höfte, H.; Gonneau, M.; Vernhettes, S. *Plant Physiol.* **2014**, *165* (4), 1521–1532.
- (22) Payyavula, R. S.; Tschaplinski, T. J.; Jawdy, S. S.; Sykes, R. W.; Tuskan, G. A.; Kalluri, U. C. Metabolic profiling reveals altered sugar and secondary metabolism in response to UGPase overexpression in *Populus*. *BMC Plant Biol.* **2014**, *14*, 265.